

**GT2011-453( +**

## **STUDY ON COMPENSATORY MAGNITUDE OF AXIAL MISALIGNMENT FOR FLEXIBLE COUPLINGS ASSEMBLED BY INTERFERENCE FIT**

**Guoping Wang**

MOE Key Laboratory for Strength and Vibration  
Xi'an Jiaotong University  
Xi'an, 710049, China

**Hualing Chen**

MOE Key Laboratory for Strength and Vibration  
Xi'an Jiaotong University  
Xi'an, 710049, China

**Shemiao Qi**

MOE Key Laboratory for  
Strength and Vibration  
Xi'an Jiaotong University  
Xi'an, 710049, China  
AVIC Harbin Dongan Engine  
(Group) Corporation Ltd.  
Harbin 150066, China

**Jiuhui Wu**

MOE Key Laboratory for  
Strength and Vibration  
Xi'an Jiaotong University  
Xi'an, 710049, China

**Lie Yu**

MOE Key Laboratory for  
Strength and Vibration  
Xi'an Jiaotong University  
Xi'an, 710049, China

### **ABSTRACT**

In general, there are three kinds of common metal flexible couplings, such as diaphragm coupling, disc coupling and gear coupling. Gear couplings, compared with diaphragm couplings and disc couplings, usually have a little ability in compensating misalignments. Diaphragm couplings have nice compensatory ability in radial, angular and axial directions, especially multi-diaphragm couplings have better compensatory ability than disc couplings. Diaphragm couplings are also suitable for higher rotating speed than disc couplings. They are high technology products, are widely used in micro gas turbine. Joint way of a diaphragm coupling with a shaft usually uses bolts and interference fit. In this article, a flexible diaphragm coupling assembled by interference fit was taken as research object. By comparing three kinds of interference assembly forms of the coupling, a most reasonable form was chosen and its axial compensatory ability was treated as main research content. An idea that "established process of balances is the varied process of misalignment magnitude" was presented. Combining the idea and the characters of interference fit, new boundary conditions were confirmed via bringing assumed shearing forces, and then the physical model was established based on the new boundary conditions mentioned above. Two-step method, based on the physical model, was presented to solve the axial compensatory magnitude. Meanwhile centrifugal stress and torsional shearing stress of diaphragms of the coupling were also considered in the

process of calculation. Finally an example was done to support the method. Some important conclusions were acquired by calculating, and they are significant for design of the flexible diaphragm couplings.

### **INTRODUCTION**

With the continuous development of high and super high speed rotating machinery, compensatory ability of misalignment in different directions is required more and more. Consequently lots of flexible couplings are invented and produced. The most famous couplings, with the largest compensatory ability, of them are flexible disc couplings and flexible diaphragm couplings. They are all suited to work at the high speed situations, so they are often applied into high-tech turbo machinery or used by the army. At present, there are just a little published journal papers and some conference papers written to describe the BENDIX diaphragm couplings[1-10] and to be used as scientific popularity in the world. The BENDIX diaphragm couplings are connected with the shaft by bolts. In this article, the main research object is a kind of special diaphragm couplings connected with shaft by interference fit and found from patents[11-13], so far there have not been relative technical papers published. This kind of diaphragm couplings is primarily used in commercially available micro gas

turbine to connect multi-span rotor and accommodate offset, angular and axial misalignments. Axial misalignment magnitude is an approaching or departing distance of two shafts connected by the diaphragm coupling, and here it is called “axial approaching misalignment” and “axial departing misalignment” respectively.

In this paper, the axial compensatory magnitude of the diaphragm coupling assembled by interference fit was studied and presented. The solving method is a kind of quantitative analysis method to the compensatory magnitude of the diaphragm coupling, and different from the qualitative analysis method by the finite element software. The effects of design parameters on the misalignment magnitude are more definite and the range of variation of the parameters is easier to define than the method by the finite element software. Thus, the method presented in this paper is more appropriate for standardization of the diaphragm coupling design.

## NOMENCLATURE

$C_{i=1,2,3,4}$  Undetermined coefficients  
 $D_0$  Diameter of the middle shaft (mm)  
 $D_1$  Anti-bending stiffness of the right diaphragm ( $N \cdot mm$ )  
 $D_2$  Anti-bending stiffness of the left diaphragm ( $N \cdot mm$ )  
 $E$  Elastic modulus of the material of the coupling ( $MPa$ )  
 $FD$  Deformation of the coupling at the first step (mm)  
 $h_1$  Thickness of the right diaphragm (mm)  
 $h_2$  Thickness of the left diaphragm (mm)  
 $l$  Length of the middle shaft (mm)  
 $M_{1r}$  Radial bending moment acted on the right diaphragm ( $N$ )  
 $M_{1\theta}$  Tangential bending moment acted on the right diaphragm ( $N$ )  
 $M_{2r}$  Radial bending moment acted on the left diaphragm ( $N$ )  
 $M_{2\theta}$  Tangential bending moment acted on the left diaphragm ( $N$ )  
 $MD$  Total axial compensatory magnitude of the “axial approaching misalignment” (mm)  
 $n$  Safety coefficient  
 $n_0$  Rotary speed of the coupling and the shaft ( $r/min$ )  
 $P_0$  Input power of the diaphragm coupling ( $kw$ )  
 $Q_d$  Tensile shearing force acted on the middle shaft ( $N/mm$ )  
 $Q_l$  Uniformly distributed shearing forces acted on the inner hole of the left diaphragm ( $N/mm$ )

$Q_r$  Uniformly distributed shearing forces acted on the inner hole of the right diaphragm ( $N/mm$ )

$Q_0$  Well-distributed shearing force acted on the inner hole of the diaphragm ( $N/mm$ )

$Q_0^{r1}$  Maximal shearing force based on the positive stress check and endured by the right diaphragm ( $N/mm$ )

$Q_0^{r2}$  Maximal shearing force based on the shearing stress check and endured by the right diaphragm ( $N/mm$ )

$Q_0^{l1}$  Maximal shearing force based on the positive stress check and endured by the left diaphragm ( $N/mm$ )

$Q_0^{l2}$  Maximal shearing force based on the shearing stress check and endured by the left diaphragm ( $N/mm$ )

$Q_{1max}$  Maximal shearing force endured by the right diaphragm ( $N/mm$ )

$Q_{2max}$  Maximal shearing force endured by the left diaphragm ( $N/mm$ )

$Q_{1r}$  Axial shearing force acted on the right diaphragm ( $N/mm$ )

$Q_{2r}$  Axial shearing force acted on the left diaphragm ( $N/mm$ )

$r$  Radial coordinate in local system on the diaphragm

$r_0$  Radius of the middle shaft (mm)

$r_{11}$  Inner radius of the left diaphragm (mm)

$r_{12}$  Outer radius of the left diaphragm (mm)

$r_{r1}$  Inner radius of the right diaphragm (mm)

$r_{r2}$  Outer radius of the right diaphragm (mm)

$SD$  Compensatory magnitude of “axial approaching misalignment” of the coupling at the second step (mm)

$T$  Torque acted on the diaphragm ( $N \cdot mm$ )

$w$  Bending deformations of the diaphragms (mm)

$w_1$  Bending deformation of the right diaphragm (mm)

$w_2$  Bending deformation of the left diaphragm (mm)

$w_{r1}$  Bending deformations of the right diaphragm caused by interference fit in the physical model (mm)

$w_{r2}$  Compensatory magnitude provided by the right diaphragm (mm)

$w'_{r2}$  Bending deformation of the right diaphragm caused by the shearing force  $Q_{1max}$  (mm)

$w_{l1}$  Bending deformations of the left diaphragm caused by interference fit in the physical model (mm)

$w_{l2}$  Compensatory magnitude provided by the left diaphragm (mm)

$w_{l_{max}}$  The deformation of the left diaphragm in the location of the inner radius (mm)  
 $z$  Axial coordinate in local system on the diaphragm  
 $dA$  The area of the differential element ( $mm^2$ )  
 $dr$  Radial width of the differential element (mm)  
 $dT$  Torque acted on the differential element ( $N \cdot mm$ )  
 $\gamma$  The shearing strain caused by torque

$\delta_d$  Tensile value of the middle shaft in the condition of  $Q_l < Q_r$  (mm)

$\delta_l$  Deformation of the left diaphragm in final equilibrium state considered effects from inertial forces and torque, but no misalignment (mm)

$\delta_p$  Compressive value of the middle shaft in the condition of  $Q_l > Q_r$  (mm)

$\delta_r$  Deformation of the right diaphragm in final equilibrium state considered effects from inertial forces and torque, but no misalignment (mm)

$\epsilon_{1r}$  Radial strain of the right diaphragm  
 $\epsilon_{1t}$  Tangential strain of the right diaphragm  
 $\mu$  Poisson's ratio of the material of the coupling

$d\sigma_{1r}$  Varied magnitude of the radial centrifugal stress thru the width of the differential element ( $MPa$ )

$\sigma_{i=1,2,3}$  Principal stress ( $MPa$ )

$\sigma_r$  The total radial stress of the right diaphragm ( $MPa$ )

$\sigma_s$  Yield limit of the material ( $MPa$ )

$\sigma_{1r}$  Radial centrifugal stress of the right diaphragm ( $MPa$ )

$\sigma_{2r}$  Radial centrifugal stress of the left diaphragm ( $MPa$ )

$\sigma_r^l$  Radial stress of the left diaphragm ( $MPa$ )

$\sigma_\theta^l$  Tangential stress of the left diaphragm ( $MPa$ )

$\sigma_r^r$  Radial stress of the right diaphragm ( $MPa$ )

$\sigma_\theta^r$  Tangential stress of the right diaphragm ( $MPa$ )

$\sigma_t$  The total tangential stress of the right diaphragm ( $MPa$ )

$\sigma_{1t}$  Tangential centrifugal stress of the right diaphragm ( $MPa$ )

$\sigma_{2t}$  Tangential centrifugal stress of the left diaphragm ( $MPa$ )

$\tau_{rz}^l$  Shearing stress of the left diaphragm ( $MPa$ )

$\tau_{rz}^r$  Shearing stress of the right diaphragm ( $MPa$ )

$\tau_{r\theta}$  Circumferential shearing stress caused by torque ( $MPa$ )

$d\phi$  The torsional angle corresponding with  $\gamma$  in the location of differential circular ring on the diaphragm ( $rad$ )

$\phi$  The torsional angle corresponding with  $\gamma$  in the location of inner radius of the diaphragm ( $rad$ )

**PHYSICAL MODEL**

As Fig.1, there are three different assembly deformation forms of diaphragms of the cup-style diaphragm coupling. Fig(a) shows the deformation form of the diaphragms when two interference fits are produced on the inner cylindrical surface of the coupling. Fig(b) shows the deformation form of the diaphragms when two interference fits are produced on the outer cylindrical surface of the coupling. Fig(c) shows the deformation form of the diaphragms when left interference fit is produced on inner cylindrical surface and right interference fit is generated on the outer cylindrical surface. Comparing Fig(a), Fig(b) and Fig(c), it's easy to know that the first one and the second one all have the best unidirectional compensatory magnitude, and the third one has better bidirectional compensatory ability, so the third one is more appropriate to be used in machinery. Here we choose the third assembly form and it is showed on the Fig.2.

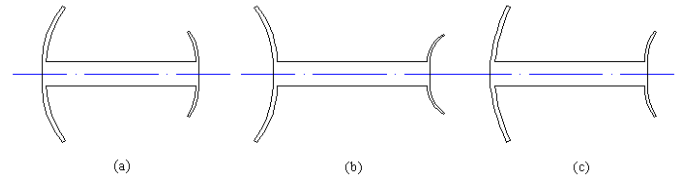


Fig.1 Different assembly deformation status of cup-style diaphragm coupling

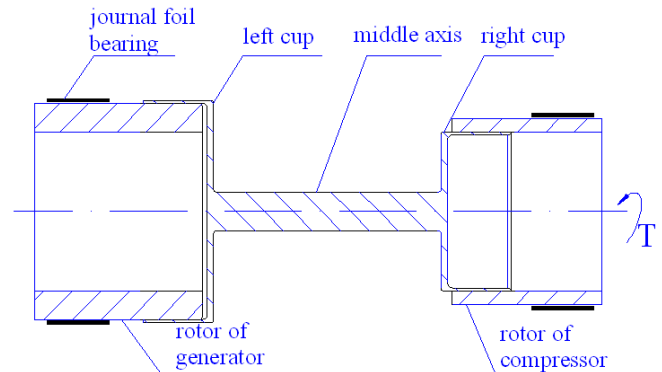


Fig.2 Better assembly form for the cup-style diaphragm coupling

With respect to the diaphragm coupling showed in Fig.2, two diaphragms generate bending deformation after assembly

and are acted by inertial force and torque at work, finally axial forces acted on the coupling are in a balance. In this balance, bending deformation of any diaphragm includes two parts: One part is caused by the final interference fit, and another part is owing to the interaction of assembly deformations of the two diaphragms. Assumed that deformations of the left diaphragm and right diaphragm are  $\delta_l$  and  $\delta_r$  respectively in the balance. When axial misalignment occurs, lead head of the coupling begins to move along the axis. Assumed that another end of the coupling is fastened, any moving distance of the lead head has a corresponding equilibrium state, so there are many equilibrium states in the moving process of the lead head. Two interference fits exist always, two diaphragms can be considered as thin annular plates with fixed outer rim and the inner surface acted by well-distributed shearing forces. In order to keep the deformations  $\delta_l$  and  $\delta_r$ , we assumed that two uniformly distributed shearing forces  $Q_l$  and  $Q_r$  act on the surface of the inner hole. According to the assumptions mentioned above, the physical model in the balance that axial misalignment does not occur is drawn, as Fig.3.

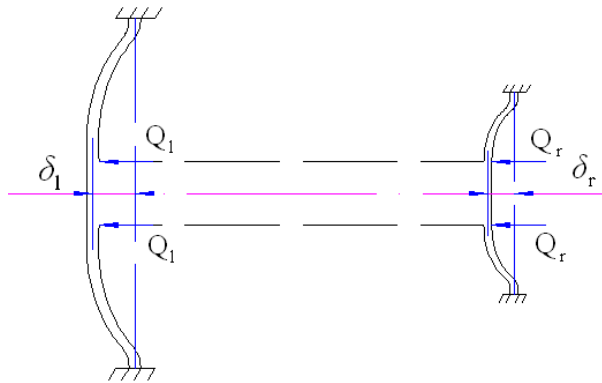


Fig.3 Physical model in the equilibrium state and no misalignment

### SOLUTION OF AXIAL MISALIGNMENT COMPENSATORY MAGNITUDE

Axial misalignment includes “axial approaching misalignment” and “axial departing misalignment”. In this paper, compensatory magnitudes were solved about the two kinds of axial misalignment. According to the physical model mentioned above, two diaphragms, acted on the surface of inner hole by shearing forces  $Q_r$  and  $Q_l$  respectively, are fixed on the outer rim. And in any balance status, the boundary conditions of the two diaphragms are always that surfaces of the inner holes are acted by shearing forces and outer rims are fastened. Just the magnitudes of the shearing forces and deformations of the diaphragms are changed in different equilibrium states. Under the balance status, if  $Q_l > Q_r$ , it can

be seen that the left cup is assembled firstly and right cup is followed, middle shaft is compressive, compression shearing force is  $Q_r$ , supposed that compressive value is  $\delta_p$ . If  $Q_l < Q_r$ , it is judged that the right cup is assembled firstly, middle shaft is in a tensile status, supposed that tensile shearing force is  $Q_d$ , tensile value is  $\delta_d$  and it is equal to  $\delta_l - \delta_r$ , then  $Q_d$  can be solved.

### AXIAL APPROACHING MISALIGNMENT

Supposed that bending deformations of the left diaphragm and the right diaphragm at the inner radius, caused by interference fit in the physical model, are  $w_{l1}$  and  $w_{r1}$ .

Assumed that the right ends of the coupling is lead head. In the equilibrium state, if  $Q_l > Q_r$ , the middle shaft is compressive. When the lead head approaches to the left end, with the increasing pressure acted on the middle shaft, the compression deformation increases. Simultaneous shearing force acted on the location of inner radius of two diaphragms also increases and until it reaches the smaller one of the maximal shearing forces endured by the two diaphragms. In this course, sum of all new deformations of the two diaphragms and the middle shaft is the axial compensatory magnitude of the “axial approaching misalignment” in the condition of  $Q_l > Q_r$ .

In the equilibrium state, if  $Q_l < Q_r$ , in order to solve the axial misalignment magnitude of the “axial approaching misalignment” more definitely, here the solving process of the total misalignment magnitude is divided into two steps. At the first step, the lead head will move three distances: the first one is decreased deformation of the middle shaft from tensile status to free status; the second one is increased deformation of the left diaphragm from  $\delta_l$  to  $w_{l1}$  as a result of disappearance of the shearing force transmitted by the middle shaft; the third distance is decreased deformation of the right diaphragm from  $\delta_r$  to  $w_{r1}$ . At the second step, the right diaphragm moves toward to the left diaphragm continuously, the free status of the middle shaft is changed into compressive status and until the transmitted shearing force reaches the smaller one of the maximal shearing forces endured by the two diaphragms, the move stops. During this moving process, sum of all new deformations based on the first step deformations is the second step deformation. Finally sum of the first step deformations and the second step deformations is the axial misalignment magnitude.

### AXIAL DEPARTING MISALIGNMENT

In the balance state, if  $Q_l < Q_r$ , the middle shaft is under tension. With the increasing tension acted on the middle shaft, the tensile deformation increases when the lead head departs from the left end. Simultaneous shearing force acted at the inner

radius of the two diaphragms also increases and until it reaches the smaller one of the maximal shearing forces endured by the two diaphragms. In this course, sum of all deformations of the two diaphragms and the middle shaft is the axial compensatory magnitude of the “axial departing misalignment” in the condition of  $Q_l < Q_r$ .

In the equilibrium state, if  $Q_l > Q_r$ , When the lead head departs from the left end, in order to solve the axial misalignment magnitude of the “axial departing misalignment” more definitely, the solving process of the total misalignment magnitudes is also divided into two steps. At the first step, the lead head will move three distances: The first one is increased deformation of the middle shaft from compressive status to free status; The second one is decreased deformation of the left diaphragm from  $\delta_l$  to  $w_{l1}$  as a result of disappearance of shearing force transmitted by the middle shaft; The third distance is increased deformation of the right diaphragm from  $\delta_r$  to  $w_{r1}$ . At the second step, the right diaphragm moves away from the left diaphragm continuously, the free status of the middle shaft is changed into tensile status and until the transmitted shearing force reaches the smaller one of the maximal shearing forces endured by the two diaphragms, the move stops. During this moving process, sum of all new deformations based on the first step deformation is the second step deformation. Finally, sum of the first step deformation and the second step deformation is the axial misalignment magnitude.

Obviously, the deformation processes in the condition of  $Q_l < Q_r$  for “axial approaching misalignment” and in condition of “ $Q_l > Q_r$ ” for “axial departing misalignment” are more general, complete and typical. Because the solving method of the misalignment magnitude in these cases is uniform, only the deformation case in condition of  $Q_l < Q_r$  for “axial approaching misalignment” is chosen to research in this article.

## ANALYSIS ON SOLUTION OF MISALIGNMENT MAGNITUDE

### Solution of the first step deformation

The left and the right diaphragms are treated as annular thin plates that their outer rims are fixed and their inner surfaces are acted by even-distributed shearing forces, and angle of rotation is zero in the position of the inner radius when bending deformation occurs. Here the right diaphragm is taken as an example to solve axial compensatory magnitude of the “axial approaching misalignment”. Supposed that  $w$  is bending deformation of the diaphragm and subscript 1 and 2 of  $w$  express the right diaphragm and the left diaphragm respectively.  $r_{11}$ ,  $r_{12}$ ,  $M_{2r}$ ,  $M_{2\theta}$  and  $Q_{2r}$  indicate inner radius,

outer radius, radial bending moment, tangential bending moment and axial shearing force on the left diaphragm.  $\sigma_r^l$ ,  $\sigma_\theta^l$  and  $\tau_{rz}^l$  are the radial stress, the tangential stress and the shearing stress corresponding with  $M_{2r}$ ,  $M_{2\theta}$  and  $Q_{2r}$ .  $r_{r1}$ ,  $r_{r2}$ ,  $M_{1r}$ ,  $M_{1\theta}$  and  $Q_{1r}$  indicate inner radius, outer radius, radial bending moment, tangential bending moment and axial shearing force on the right diaphragm,  $\sigma_r^r$ ,  $\sigma_\theta^r$  and  $\tau_{rz}^r$  are the radial stress, the tangential stress and the shearing stress corresponding with  $M_{1r}$ ,  $M_{1\theta}$  and  $Q_{1r}$ .  $h_1$  and  $h_2$  are the thickness of the right diaphragm and the left diaphragm respectively.  $D_1$  and  $D_2$  are the anti-bending stiffness of right diaphragm and left diaphragm respectively.  $z$  is the axial coordinate in local system on the diaphragm. Origin of the local system is located at the center of the mid-surface of the diaphragm. According to the theory of plate and shell[14], bending displacement, bending moment, shearing force and stress of the right diaphragm are expressed as follows:

$$w_1(r) = C_1 \ln \frac{r}{r_2} + C_2 \left(\frac{r}{r_1}\right)^2 \ln \frac{r}{r_1} + \frac{1}{2} C_3 \left[\left(\frac{r}{r_1}\right)^2 - 1\right] + C_4 \quad (1)$$

$$M_{1r} = -D_1 \left( \frac{d^2 w_1}{dr^2} + \frac{\mu}{r} \frac{dw_1}{dr} \right) \quad (2)$$

$$M_{1\theta} = -D_1 \left( \mu \frac{d^2 w_1}{dr^2} + \frac{1}{r} \frac{dw_1}{dr} \right) \quad (3)$$

$$Q_{1r} = D_1 \left( \frac{d^3 w_1}{dr^3} + \frac{1}{r} \frac{d^2 w_1}{dr^2} - \frac{1}{r^2} \frac{dw_1}{dr} \right) \quad (4)$$

$$\sigma_r^r = \frac{12 M_{1r} z}{h_1^3} \quad (5)$$

$$\sigma_\theta^r = \frac{12 M_{1\theta} z}{h_1^3} \quad (6)$$

$$\tau_{rz}^r = \frac{6 Q_{1r}}{h_1^3} \left( \frac{h_1^2}{4} - z^2 \right) \quad (7)$$

Boundary conditions are as follows:

$$Q_{1r} \Big|_{r=r_{r1}} = Q_r; \quad \frac{dw_1}{dr} \Big|_{r=r_{r1}} = 0;$$

$$w_1 \Big|_{r=r_{r2}} = 0; \quad \frac{dw_1}{dr} \Big|_{r=r_{r2}} = 0 \quad (8)$$

From equation (1) thru equation (8), the equation of  $Q_r$  acted on the inner hole surface of the right diaphragm and bending deformation  $\delta_r$  is as follows:

$$Q_r = \frac{-8\delta_r D_1 (r_{r2}^2 - r_{r1}^2)}{r_{r1} [-4r_{r1}^2 r_{r2}^2 (\ln \frac{r_{r2}}{r_{r1}})^2 - 2r_{r1}^2 r_{r2}^2 + r_{r1}^4 + r_{r2}^4]} \quad (9)$$

Similarly, the equation of  $Q_l$  and  $\delta_l$  is as follows:

$$Q_l = \frac{-8\delta_l D_2 (r_{l2}^2 - r_{l1}^2)}{r_{l1} [-4r_{l1}^2 r_{l2}^2 (\ln \frac{r_{l2}}{r_{l1}})^2 - 2r_{l1}^2 r_{l2}^2 + r_{l1}^4 + r_{l2}^4]} \quad (10)$$

Bending deformations  $\delta_l$  and  $\delta_r$  are taken as the known conditions to be provided in this paper. Comparing the magnitude of  $Q_l$  and  $Q_r$  by equation (9) and (10), deformation status and deformation magnitude of the middle shaft can be obtained. And then, shearing force transmitted by the middle shaft is also solved. Subsequently, the first part deformations of the diaphragms caused by interference fit and the second part deformations caused by interaction of the first part deformations can be solved. With respect to ‘‘axial approaching misalignment’’, we supposed that the tensile shearing force acted on the middle shaft is  $Q_d$  in the condition of  $Q_l < Q_r$ , and the radius of the middle shaft is  $r_0$ . Tensile value of the middle shaft is expressed as follows:

$$\delta_d = \delta_l - \delta_r \quad (11)$$

Then, tensile shearing force is as follows:

$$Q_d = \frac{\delta_d \pi E r_0^2}{2\pi_0 l} = \frac{\delta_d E r_0}{2l} \quad (12)$$

$w_{r1}$  is the bending deformation of the right diaphragm at the inner radius caused by interference fit in the physical model and it can be achieved just in the boundary conditions of a fixed outer rim and an inner hole surface acted by shearing force  $Q_r - Q_d$ . The expression is as follows:

$$w_{r1} = \frac{(Q_r - Q_d) r_{r1}^3 r_{r2}^2}{2D_1 (r_{r2}^2 - r_{r1}^2)} [\ln(\frac{r_{r2}}{r_{r1}})]^2 - \frac{r_{r1} (r_{r2}^2 - r_{r1}^2) (Q_r - Q_d)}{8D_1} \quad (13)$$

As a result of disappearance of shearing force transmitted by the middle shaft, decreased deformation of the left diaphragm from  $\delta_r$  to  $w_{r1}$  is  $\delta_r - w_{r1}$ . Similarly,  $w_{l1}$  of the left diaphragm can be achieved just in the boundary condition of a fixed outer rim and an inner hole surface acted by shearing force  $Q_r + Q_d$ . The expression is as follows:

$$w_{l1} = \frac{(Q_l + Q_d) r_{l1}^3 r_{l2}^2}{2D_1 (r_{l2}^2 - r_{l1}^2)} [\ln(\frac{r_{l2}}{r_{l1}})]^2 - \frac{r_{l1} (r_{l2}^2 - r_{l1}^2) (Q_l + Q_d)}{8D_1} \quad (14)$$

So increased deformation of the left diaphragm from  $\delta_l$  to  $w_{l1}$  is  $w_{l1} - \delta_l$ . As a result, all three deformations included in the first step deformation have been obtained.

Assumed the first step deformation is  $FD$ , then the expression is as follows:

$$\begin{aligned} FD &= w_{l1} - \delta_l + \delta_d + \delta_r - w_{r1} \\ &= \frac{(Q_l + Q_d) r_{l1}^3 r_{l2}^2}{2D_1 (r_{l2}^2 - r_{l1}^2)} [\ln(\frac{r_{l2}}{r_{l1}})]^2 - \frac{r_{l1} (r_{l2}^2 - r_{l1}^2) (Q_l + Q_d)}{8D_1} \\ &\quad - \frac{(Q_r - Q_d) r_{r1}^3 r_{r2}^2}{2D_1 (r_{r2}^2 - r_{r1}^2)} [\ln(\frac{r_{r2}}{r_{r1}})]^2 + \frac{r_{r1} (r_{r2}^2 - r_{r1}^2) (Q_r - Q_d)}{8D_1} \end{aligned} \quad (15)$$

## MAXIMAL SHEARING FORCE ENDURED BY THE DIAPHRAGM

Maximal shearing force endured by the diaphragm in the physical model may be affected by bending stress, shearing stress caused by interference fit, inertial stress and torsional stress. According to the distributions of all kinds of stresses, the first step is to judge the critical section and critical points on the section; the second step is to check the positive stress and shearing stress at their critical points respectively. Solved shearing force at the critical status of material yield limit is the maximal shearing force endured by diaphragm at the inner radius.

### Centrifugal stress analysis

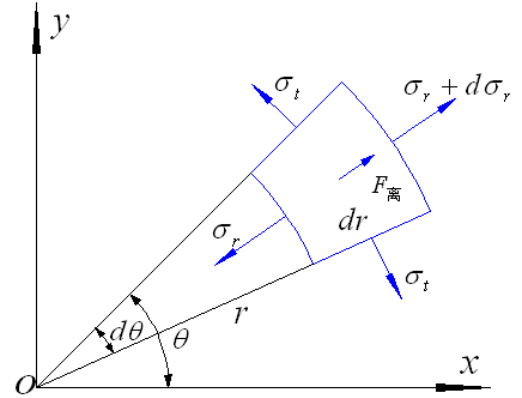


Fig.4 Centrifugal stress analysis

Here a differential element on the right diaphragm is taken just as Fig.4. Its radial width is  $dr$ , the thickness of the diaphragm is  $h_1$ , the radial stress is  $\sigma_{1r}$  in the location of  $r$  and radial stress is  $\sigma_{1r} + d\sigma_{1r}$  in the location of  $r + dr$ , tangential stress on the differential element is  $\sigma_{1t}$ . Equation of the stress equilibrium is expressed as follows:

$$\frac{d\sigma_{1r}}{dr} + \frac{\sigma_{1r} - \sigma_{1t}}{r} + \rho\omega^2 r = 0 \quad (16)$$

According to the stress function method,  $\sigma_{1r}$  and  $\sigma_{1t}$  can be solved as follows:

$$\sigma_{1r} = C_1 + \frac{C_2}{r^2} - \frac{(3 + \mu)}{8} \rho \omega^2 r^2 \quad (17)$$

$$\sigma_{1t} = C_1 - \frac{C_2}{r^2} - \frac{(1 + 3\mu)}{8} \rho \omega^2 r^2 \quad (18)$$

Thin annular plate can be seen as plane stress problem, so the constitutive equations[15] are as follows:

$$\begin{aligned} \varepsilon_{1r} &= \frac{1}{E} (\sigma_{1r} - \mu \sigma_{1t}) \\ \varepsilon_{1t} &= \frac{1}{E} (\sigma_{1t} - \mu \sigma_{1r}) \end{aligned} \quad (19)$$

Geometric equations are as follows:

$$\varepsilon_{1r} = \frac{dw_1}{dr}, \quad \varepsilon_{1t} = \frac{w_1}{r} \quad (20)$$

Boundary conditions are as follows:

$$w_1 \Big|_{r=r_{r1}} = 0; \quad \frac{dw_1}{dr} \Big|_{r=r_{r1}} = 0 \quad (21)$$

Combining equation (16)~(20), centrifugal stresses on the right diaphragm are expressed as follows:

$$\sigma_{1r} = \frac{1}{8} \rho r_{r1}^2 \omega^2 \left[ 2(\mu + 1) - \frac{r_{r1}^2 (\mu - 1)}{r^2} - \frac{(3 + \mu) r^2}{r_{r1}^2} \right] \quad (22)$$

$$\sigma_{1t} = \frac{1}{8} \rho r_{r1}^2 \omega^2 \left[ 2(\mu + 1) + \frac{r_{r1}^2 (\mu - 1)}{r^2} - \frac{(1 + 3\mu) r^2}{r_{r1}^2} \right] \quad (23)$$

Similarly, centrifugal stress on the left diaphragm can be expressed as follows:

$$\sigma_{2r} = \frac{1}{8} \rho r_{l1}^2 \omega^2 \left[ 2(\mu + 1) - \frac{r_{l1}^2 (\mu - 1)}{r^2} - \frac{(3 + \mu) r^2}{r_{l1}^2} \right] \quad (24)$$

$$\sigma_{2t} = \frac{1}{8} \rho r_{l1}^2 \omega^2 \left[ 2(\mu + 1) + \frac{r_{l1}^2 (\mu - 1)}{r^2} - \frac{(1 + 3\mu) r^2}{r_{l1}^2} \right] \quad (25)$$

It can be seen from equation (22)~(25) that centrifugal stresses is zero in the location of inner radius of the diaphragm and is maximal in the outer rim of the diaphragm.

### Shearing stress analysis caused by torque

Common torsions almost are torsions of rotating shafts and the torque is transmitted along the axis. In this paper, the torque is transmitted along the radial direction of the diaphragm from inner radius to outer radius or from outer radius to inner radius, but torsional shearing stress is uniform. Here the style of transmission torque from inner radius to outer radius is taken to research in this paper, as Fig.5.  $\gamma$  is the shearing strain caused by torque and  $\phi$  is torsional angle corresponding with  $\gamma$  at the inner radius of the diaphragm. A differential circular ring is taken in the location of  $r$  and its width is  $dr$  along the radial direction. Shearing strain on the differential circular ring is  $\gamma$

too, and torsional angle is  $d\phi$ . The thickness of the diaphragm is  $h_1$ .

Supposed that circumferential shearing stress caused by torque is  $\tau_{r\theta}$ . A differential element was taken on the differential circular ring along the circumferential direction and the area of the differential element is  $dA$ . So torque acted on the differential element is expressed as follows:

$$dT = \tau_{r\theta} r dA$$

Integrating to above equation, the following equation can be obtained:

$$T = \int \tau_{r\theta} r dA = 2\pi r^2 h_1 \tau_{r\theta} \quad (26)$$

So, shearing stress can be expressed as follows:

$$\tau_{r\theta} = \frac{T}{2\pi r^2 h_1} \quad (27)$$

It can be seen that shearing stress generated by torque on the diaphragm is decreasing along the radius from inner radius to outer radius.

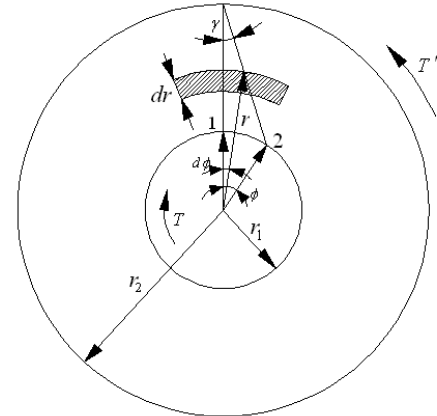


Fig.5 Torsional deformation of the diaphragm

### Solution of the maximal shearing force endured by diaphragm

We assumed that a well-distributed shear force  $Q_0$  is acted on the inner hole surface of the diaphragm. Misalignment deformation process in every moment can be treated as a equilibrium state. For example, the physical model is the original balance. Thus, every diaphragm can be simplified into a thin annular plate and the boundary condition is uniform in every equilibrium state. At the outer radius, the boundary condition is that displacement and angle of rotation are zero. At the inner radius, angle of rotation is zero too and a shearing force is acted on the inner hole surface, here the shearing force is  $Q_0$ . So the boundary conditions are shown as follows:

$$Q_{1r} = \left|_{r=r_{r1}} = Q_0; \quad \frac{dw_1}{dr} \Big|_{r=r_{r1}} = 0; \right.$$

$$w_1 \Big|_{r=r_{r2}} = 0; \quad \frac{dw_1}{dr} \Big|_{r=r_{r2}} = 0 \quad (28)$$

Combining the equations (1)~(7), bending stresses on the diaphragm are as follows:

$$\sigma_r^r = \frac{6Q_0 r_{r1} z}{h_1^3 (r_{r1}^2 - r_{r2}^2)} \left\{ \frac{r_{r1}^2 r_{r2}^2 (1 - \mu)}{r^2} \ln\left(\frac{r_2}{r_1}\right) \right.$$

$$\left. + [(r_{r1}^2 - r_{r2}^2)(1 + \mu) \ln\left(\frac{r}{r_1}\right) + r_{r1}^2 - r_{r2}^2 + (1 + \mu)r_{r2}^2 \ln\left(\frac{r_2}{r_1}\right)] \right\} \quad (29)$$

$$\sigma_\theta^r = \frac{6Q_0 r_{r1} z}{h_1^3 (r_{r1}^2 - r_{r2}^2)} \left\{ \frac{r_{r1}^2 r_{r2}^2 (\mu - 1)}{r^2} \ln\left(\frac{r_2}{r_1}\right) \right.$$

$$\left. + [(1 + \mu)(r_{r1}^2 - r_{r2}^2) \ln\left(\frac{r}{r_1}\right) + \mu(r_{r1}^2 - r_{r2}^2) + (1 + \mu)r_{r2}^2 \ln\left(\frac{r_2}{r_1}\right)] \right\} \quad (30)$$

$$\tau_{rz}^r = \frac{3Q_0 r_{r1}}{2h_1^3 r} (h_1^2 - 4z^2) \quad (31)$$

Using above method, parameters of the right diaphragm are substituted into parameters of the left diaphragm in the equations (29), (30) and (31), distribution of bending stresses of the left diaphragm is obtained. Using the equations (22), (23), (29) and (30), total radial stress  $\sigma_r$  and tangential stress  $\sigma_t$  are expressed as follows:

$$\sigma_r = \sigma_{1r} + \sigma_r^r$$

$$= \frac{1}{8} \rho r_{r1}^2 \omega^2 \left[ 2(\mu + 1) - \frac{r_{r1}^2 (\mu - 1)}{r^2} - \frac{(3 + \mu)r^2}{r_{r1}^2} \right]$$

$$+ \frac{6Q_0 r_{r1} z}{h_1^3 (r_{r1}^2 - r_{r2}^2)} \left\{ \frac{r_{r1}^2 r_{r2}^2 (1 - \mu)}{r^2} \ln\left(\frac{r_2}{r_1}\right) \right.$$

$$\left. + [(r_{r1}^2 - r_{r2}^2)(1 + \mu) \ln\left(\frac{r}{r_1}\right) \right.$$

$$\left. + r_{r1}^2 - r_{r2}^2 + (1 + \mu)r_{r2}^2 \ln\left(\frac{r_2}{r_1}\right)] \right\} \quad (32)$$

$$\sigma_t = \sigma_{1t} + \sigma_\theta^r$$

$$= \frac{1}{8} \rho r_{r1}^2 \omega^2 \left[ 2(\mu + 1) + \frac{r_{r1}^2 (\mu - 1)}{r^2} - \frac{(1 + 3\mu)r^2}{r_{r1}^2} \right]$$

$$+ \frac{6Q_0 r_{r1} z}{h_1^3 (r_{r1}^2 - r_{r2}^2)} \left\{ \frac{r_{r1}^2 r_{r2}^2 (\mu - 1)}{r^2} \ln\left(\frac{r_2}{r_1}\right) \right.$$

$$\left. + [(1 + \mu)(r_{r1}^2 - r_{r2}^2) \ln\left(\frac{r}{r_1}\right) \right.$$

$$\left. + \mu(r_{r1}^2 - r_{r2}^2) + (1 + \mu)r_{r2}^2 \ln\left(\frac{r_2}{r_1}\right)] \right\} \quad (33)$$

According to the equations (27), (31), (32) and (33), distributed drawing of the positive stress and shearing stress can be obtained. And then, positions of the critical section and critical point on the section can be judged. At the critical point,

material strength is checked with respect to positive stress and shearing stress, it was based on the third strength theory[16]. Generally speaking, solved maximal shearing forces are different based on positive stress check and shearing stress check, and the smaller value of the solved maximal shearing forces is taken as maximal shearing force endured by diaphragm. Here supposed that the maximal shearing force endured by the right diaphragm is  $Q_{1\max}$  and the maximal shearing force endured by the left diaphragm is  $Q_{2\max}$ .

### SOLUTION OF THE SECOND STEP COMPENSATORY MAGNITUDE

Comparing the magnitude of  $Q_{1\max}$  and  $Q_{2\max}$ , if  $Q_{1\max} > Q_{2\max}$ , the middle shaft changes its free status into compressive status, when approaching move of the lead head at the second step, based on the approaching move at the first step, occurs. In this case, the shearing force transmitted by middle shaft uses  $Q_{2\max}$  when the material strength is checked. Then the new deformations of two diaphragms and the middle shaft can be solved, i.e. compensatory magnitude of the approaching move at the second step is obtained.

If  $Q_{1\max} < Q_{2\max}$ , after the first approaching move, the current deformation of the right diaphragm can be seen as the deformation acted by shearing force  $Q_r - Q_d$  and it is  $w_{r1}$ . With the move of the right diaphragm at the second step, the deformation status of the diaphragm will be a completely reversed deformation status finally. In this case, the force transmitted by the middle shaft uses  $Q_{1\max} + Q_r - Q_d$  when the material strength is checked, but the transmitted shearing force must meet the condition of  $Q_{1\max} + Q_r - Q_d < Q_{2\max}$ . If  $Q_{1\max} + Q_r - Q_d > Q_{2\max}$ , the force transmitted by middle shaft uses  $Q_{2\max}$  when material strength is checked. Aiming at the two cases above, an exact analysis is presented as follows:

#### Compressive deformation of the middle shaft $\delta_p$

If  $Q_{1\max} + Q_r - Q_d < Q_{2\max}$ ,

$$\delta_p = \frac{2l(Q_{1\max} + Q_r - Q_d)}{Er_0} \quad (34)$$

If  $Q_{1\max} + Q_r - Q_d > Q_{2\max}$ ,

$$\delta_p = \frac{2lQ_{2\max}}{Er_0} \quad (35)$$

#### Deformation of the left diaphragm $w_{l2}$

If  $Q_{1\max} + Q_r - Q_d < Q_{2\max}$ , the shearing force acted on the surface of inner hole is  $Q_{1\max} + Q_r - Q_d$ . Supposed that the deformation of the left diaphragm at the inner radius is  $w_{l\max}$ . In this case, compensatory magnitude provided by the left diaphragm is  $w_{l2} = w_{l\max} - w_{l1}$ .

$$w_{l\max} = \frac{(Q_{1\max} + Q_r - Q_d)r_{l1}^3r_{l2}^2[\ln(\frac{r_{l2}}{r_{l1}})]^2}{2D_2(r_{l2}^2 - r_{l1}^2)} - \frac{r_{l1}(r_{l2}^2 - r_{l1}^2)(Q_{1\max} + Q_r - Q_d)}{8D_2} \quad (36)$$

Combining equations (14) and (35),  $w_{l2}$  is expressed as follows:

$$w_{l2} = \frac{(Q_{1\max} + Q_r - Q_l)r_{l1}^3r_{l2}^2[\ln(\frac{r_{l2}}{r_{l1}})]^2}{2D_2(r_{l2}^2 - r_{l1}^2)} - \frac{r_{l1}(r_{l2}^2 - r_{l1}^2)(Q_{1\max} + Q_r - Q_l)}{8D_2} - \frac{(Q_l + Q_d)r_{l1}^3r_{l2}^2[\ln(\frac{r_{l2}}{r_{l1}})]^2}{2D_1(r_{l2}^2 - r_{l1}^2)} + \frac{r_{l1}(r_{l2}^2 - r_{l1}^2)(Q_l + Q_d)}{8D_1} \quad (37)$$

If  $Q_{1\max} + Q_r - Q_d > Q_{2\max}$ , the shearing force transmitted by the middle shaft is  $Q_{2\max}$ , so here  $w_{l\max}$  and  $w_{l2}$  are expressed as follows:

$$w_{l\max} = \frac{Q_{2\max}r_{l1}^3r_{l2}^2[\ln(\frac{r_{l2}}{r_{l1}})]^2}{2D_2(r_{l2}^2 - r_{l1}^2)} - \frac{r_{l1}(r_{l2}^2 - r_{l1}^2)Q_{2\max}}{8D_2} \quad (38)$$

$$w_{l2} = \frac{Q_{2\max}r_{l1}^3r_{l2}^2[\ln(\frac{r_{l2}}{r_{l1}})]^2}{2D_2(r_{l2}^2 - r_{l1}^2)} - \frac{r_{l1}(r_{l2}^2 - r_{l1}^2)Q_{2\max}}{8D_2} - \frac{(Q_l + Q_d)r_{l1}^3r_{l2}^2[\ln(\frac{r_{l2}}{r_{l1}})]^2}{2D_1(r_{l2}^2 - r_{l1}^2)} + \frac{r_{l1}(r_{l2}^2 - r_{l1}^2)(Q_l + Q_d)}{8D_1} \quad (39)$$

### Deformation of the right diaphragm $w_{r2}$

If  $Q_{1\max} + Q_r - Q_d < Q_{2\max}$ ,

Here the shearing force transmitted by the middle shaft is  $Q_{1\max} + Q_r - Q_d$ . With respect to the right diaphragm, there are two uniformly distributed shearing force acted on the surface of the inner hole, and they have different directions, so the move deformation of the right diaphragm at the second step can use two parts of deformations to express, i.e one part is  $w_{r1}$  and another deformation is  $w'_{r2}$  caused by shearing force  $Q_{1\max}$ . Thus,

$$w_{r2} = w'_{r2} + w_{r1}$$

$$w'_{r2} = \frac{Q_{1\max}r_{r1}^3r_{r2}^2[\ln(\frac{r_{r2}}{r_{r1}})]^2}{2D_1(r_{r2}^2 - r_{r1}^2)} - \frac{r_{r1}Q_{1\max}(r_{r2}^2 - r_{r1}^2)}{8D_1} \quad (40)$$

Combining equations (13) and (40), the deformation of the right diaphragm  $w_{r2}$  is solved as the following formula:

$$w_{r2} = \frac{(Q_{1\max} + Q_r - Q_d)r_{r1}^3r_{r2}^2[\ln(\frac{r_{r2}}{r_{r1}})]^2}{2D_1(r_{r2}^2 - r_{r1}^2)} - \frac{r_{r1}(r_{r2}^2 - r_{r1}^2)(Q_{1\max} + Q_r - Q_d)}{8D_1} \quad (41)$$

If  $Q_{1\max} + Q_r - Q_d > Q_{2\max}$ , the differences from the former is that deformation  $w'_{r2}$  is caused by shearing force  $Q_{2\max} - Q_r + Q_d$ , so the results of  $w'_{r2}$  and  $w_{r2}$  in this condition are expressed respectively as follows:

$$w'_{r2} = \frac{(Q_{2\max} - Q_r + Q_d)r_{r1}^3r_{r2}^2[\ln(\frac{r_{r2}}{r_{r1}})]^2}{2D_1(r_{r2}^2 - r_{r1}^2)} - \frac{r_{r1}(Q_{2\max} - Q_r + Q_d)(r_{r2}^2 - r_{r1}^2)}{8D_1} \quad (42)$$

$$w_{r2} = \frac{Q_{2\max}r_{r1}^3r_{r2}^2[\ln(\frac{r_{r2}}{r_{r1}})]^2}{2D_1(r_{r2}^2 - r_{r1}^2)} - \frac{r_{r1}Q_{2\max}(r_{r2}^2 - r_{r1}^2)}{8D_1} \quad (43)$$

Considering the mentioned above, we assumed that approaching compensatory magnitude at the second step is  $SD$ , and then the expression of  $SD$  is as follows:

$$SD = \delta_p + w_{l2} + w_{r2} \quad (44)$$

The flow chart of the solving method and steps is seen from ANNEX B.

### CALCULATION EXAMPLE

Supposed that a group of parameters of the diaphragm coupling are as the Table1.(Seen from ANNEX A, Table.1)

With respect to  $\delta_l$  and  $\delta_r$ , they can be done special calculation in considering of assembly, rotating speed and temperature, here just for telling the solving method of the misalignment compensatory magnitude, so the value of  $\delta_l$  and  $\delta_r$  are presented without any calculation.

### SOLUTION OF COMPENSATORY MAGNITUDE OF THE RIGHT DIAPHRAGM AT THE FIRST STEP

Substituting  $\delta_l = 0.104$  and  $\delta_r = 0.1$  into equations (9) and (10), the assumed shearing force are  $Q_l = -26.4411\text{N}$  and  $Q_r = -44.1753\text{N}$ . Apparently their magnitude meets the condition of  $Q_l < Q_r$ . So approaching

misalignment magnitude at the first step and its three parts are calculated according to equations (11)~(15) just as follows:

$$\delta_d = \delta_l - \delta_r = 0.004 \text{ mm}$$

$$Q_d = \frac{\delta_d E r_0}{2l} = 18.7755 N$$

In order to keep uniform sign of the input shearing force on the diaphragm, we take the shearing force acted in the reverse direction negative value, i.e.  $Q_d = -18.7755 N$ . According to the equation (13), the value of  $w_{r1}$  is as follows:

$$w_{r1} = 0.0575 \text{ mm}$$

And,

$$\delta_r - w_{r1} = 0.0425 \text{ mm}$$

According to the equation (14), the value of  $w_{l1}$  is as follows:

$$w_{l1} = 0.17 \text{ mm}$$

And,

$$w_{l1} - \delta_l = 0.066 \text{ mm}$$

Thus,

$$\begin{aligned} FD &= w_{l1} - \delta_l + \delta_d + \delta_r - w_{r1} \\ &= 0.066 + 0.0425 + 0.004 \\ &= 0.1125 \text{ mm} \end{aligned}$$

### SOLUTION OF THE MAXIMAL SHEARING FORCE ENDURED BY THE DIAPHRAGMS

Known from equations (31), (32) and (33), critical section on the diaphragm is located at  $r = r_{r1}$ , i.e. critical section is the surface of the inner hole of the diaphragm. Critical point corresponding with the shearing stress is located in the section of  $z = 0$ . Critical point corresponding with the positive stress is located in the section of  $z = h_1 / 2$ .

Firstly, checking on the positive stress, order that

$$\sigma_1 = |\sigma_r| = |\sigma_r(r = r_{r1}, z = h_1 / 2)|, \quad \sigma_2 = 0,$$

$$\sigma_3 = |\sigma_t| = |\sigma_t(r = r_{r1}, z = h_1 / 2)|, \quad (45)$$

According to equations (32) and (33), positive stresses on the critical point are expressed as follows:

$$\sigma_r(r = r_{r1}, z = h_1 / 2) = \frac{3Q_0 r_{r1}}{h_1^2 (r_{r1}^2 - r_{r2}^2)} [2r_{r2}^2 \ln(\frac{r_2}{r_1}) + r_{r1}^2 - r_{r2}^2] \quad (46)$$

$$\sigma_t(r = r_{r1}, z = h_1 / 2) = \frac{3\mu Q_0 r_{r1}}{h_1^2 (r_{r1}^2 - r_{r2}^2)} [2r_{r2}^2 \ln(\frac{r_2}{r_1}) + (r_{r1}^2 - r_{r2}^2)] \quad (47)$$

Make check about positive stress based on the third strength theory:

$$|\sigma_1 - \sigma_3| \leq \frac{\sigma_s}{n} = [\sigma] \quad (48)$$

According to equation (48), maximal shearing force based on the positive stress check and endured by the right diaphragm is  $|Q_0^{r1}| = 53.1861 N$ . Similarly, maximal shearing force based on the positive stress check and endured by the left diaphragm is  $|Q_0^{l1}| = 55.7368 N$ .

Secondly, checking on shearing stress and meeting the following conditions:

$$\tau_{r\theta}|_{r=r_{r1}} = \frac{T}{2\pi r^2 h_1} = \frac{9550 P_0}{2\pi r^2 h_1 n_0} = 0.1373 \leq \frac{\sigma_s}{2n} = 343.75$$

$$|\tau_{rz}(r = r_{r1}, z = 0)| \leq \frac{\sigma_s}{2n} \quad (49)$$

Combining equation (31) and (49), maximal shearing force based on the shearing stress check and endured by the right diaphragm is  $|Q_0^{r2}| = 458.3333 N$ . The maximal shearing force based on the shearing stress check and endured by the left diaphragm is  $|Q_0^{l2}| = 550 N$ . So we choose the smaller value of the maximal shearing forces with respect to every diaphragm, the maximal shearing force of the right diaphragm at the inner radius should be  $|Q_{1\max}| = 53.1861 N$ , and the maximal shearing force of the left diaphragm at the inner radius should be  $|Q_{2\max}| = 55.7368 N$ .

Obviously,

$$|Q_{1\max}| < |Q_{2\max}| \text{ and } |Q_{1\max} + Q_r - Q_d| > |Q_{2\max}|.$$

### SOLUTION OF APPROACHING COMPENSATORY MAGNITUDE AT THE SECOND STEP

According to equation (35), compressive magnitude of the middle shaft at the second step is as follows:

$$\delta_p = \frac{2 \times 49 \times (-55.7368)}{115 \times 10^3 \times 4} = -0.0119 \text{ mm}$$

Obviously,

$$|Q_{1\max} + Q_r - Q_d| = 78.5859 > |Q_{2\max}| = 55.7368$$

In this case, shearing force transmitted by the middle shaft is

$$Q_d = Q_{2\max} = -55.7368 N$$

Deformation of the left diaphragm is as follows:

$$w_{l\max} = 0.2192 \text{ mm}$$

$$w_{l1} = 0.17 \text{ mm}$$

$$w_{l2} = w_{l\max} - w_{l1} = 0.0492 \text{ mm}$$

Deformation of the right diaphragm is as follows:

$$w'_{r2} = 0.0687 \text{ mm}$$

$$w_{r1} = 0.0575 \text{ mm}$$

$$w_{r2} = w'_{r2} + w_{r1} = 0.1262\text{mm}$$

So the compensatory magnitude at the second step is as follows:

$$\begin{aligned} SD &= |w_{l2}| + |\delta_p| + |w_{r2}| \\ &= 0.0492 + 0.0119 + 0.1262 \\ &= 0.1873\text{mm} \end{aligned}$$

Above all, total compensatory magnitude  $MD$  of “axial approaching misalignment” in the provided conditions of calculation example is as follows:

$$\begin{aligned} MD &= FD + SD \\ &= 0.1125 + 0.1873 \\ &= 0.2998\text{mm} \end{aligned}$$

According to the text above, the axial compensatory magnitude of the “axial approaching misalignment” has been solved, the two-step method is convenient and valid, but the parameters in the calculation example are not the best parameters, so the result of misalignment magnitude doesn't achieve the maximal compensatory value.

## CONCLUSION

Above all, via comparing the deformation forms of the two diaphragms in different assembly ways between the diaphragm coupling and two sides rotating shaft, a kind of deformation form was chosen based on the bidirectional requirement of axial misalignment compensation. The right end of the coupling was treated as lead head when the axial misalignment occurs, i.e. the right end of the coupling is connected with a drive shaft. The diaphragms were seen as annular thin plate. An idea that the process of establishing the equilibrium states is the varied process of the misalignment compensatory magnitude was presented. Two frictional shearing forces acted at inner radius of the diaphragms were put forward and the physical model was established based on an assumption that interference fit is fixed connection and a condition that bending deformation must be kept in the equilibrium state. And then, two-step method of solving the axial misalignment magnitude based on the physical model was presented. As a result of the same solving principle of the two directions misalignments, “axial approaching misalignment” was chosen to do exact analysis. Calculation formulas of the axial compensatory magnitude, based on the acquirement of maximal shearing force acted at the inner radius of the diaphragm, were presented at the first step and the second step. Finally, a calculation example was presented and used to calculate the axial approaching misalignment magnitude in the condition of the known parameters, and some conclusions can be obtained by the calculation and analysis above.

1) According to the two-step method presented above, axial misalignment compensatory magnitudes of the diaphragm coupling at the first and the second step are easy to solve, but whether the second step axial compensatory magnitude can

obtain the maximal value or not, is strongly depended on the matching of the design parameters of the two diaphragms, and the best parameters can be obtained by calculating more than once.

2) On the diaphragm, the maximal radial bending stress occurs on both sides of the surface and at the inner radius, the maximal tangential bending stress occurs on the both sides of the surface and near the location of the inner radius. They usually decided the main distribution of the stresses and the location of the critical section on the diaphragm. The maximal shearing stress occurs on the middle surface of the diaphragm and at the inner radius. The maximal value of the torsional shearing stress is also on the surface of the inner hole, but they are far smaller than the positive stresses, so they don't have enough effects on the strength of the diaphragm. The maximal value of the centrifugal stress is on the outer rim of the diaphragm, and its magnitude is smaller than the maximal value of the bending stress, so it also can't change the position of the critical section.

3) The outer radius and the thickness of the diaphragm are the main influencing factors on the axial compensation ability of the coupling. Geometric sizes of the middle shaft have a little effect on the axial compensation value. With the increase of the outer radius of the diaphragm and the length of the middle shaft, the axial compensation magnitude is increasing. With the increase of the thickness of the diaphragm and the radius of the middle shaft, the axial compensation magnitude is decreasing. Where, the change of the axial compensation magnitude is most sensitive to the change of the thickness of the diaphragm.

## ACKNOWLEDGMENTS

The work described in this paper was supported by the National High-tech Research and Development Program of China (Grant No. 2007AA050501).

## REFERENCES

- [1] Zhu Keke, Zhu Rupeng, “An Analytic Solution to the Unsymmetrical Bending Problem of Diaphragm Coupling”, *Applied Mathematics and Mechanics*, 29(12), 2008, pp1643-1649. (In Chinese)
- [2] Xuan Qi, Guo Hui, “Relations between force and torque on the disk of elastic diaphragm coupling”, *Journal of machine design and manufacture*, 4, 2008, pp85-87. (In Chinese)
- [3] Ai Pinggui, Zhu rupeng, “Stress and modal analysis for the disk of elastic diaphragm coupling by ANSYS”, *Journal of machine engineering*, 1, Dec. 2008, pp124-125. (In Chinese)
- [4] Mancuso Jon R., Zilbeman, J., et al. “Flexible-element couplings: how safe is safe?”, *Hydrocarbon Processing*, 1994, pp93-96.
- [5] Mancuso Jon R., “Just how flexible is your flexible coupling in reality?”, *World Pumps*. Sep. 2000.
- [6] Mancuso Jon R., “What are the differences in high performance flexible couplings for turbomachinery?”,

Proceeding of the thirty-second turbomachinery symposium, 2003, pp189-207.

[7] Kop-Flex Inc, “Flexible diaphragm coupling: MS Marine Style”, Emerson Industrial Automation, 2003.

[8] Mancuso Jon R., “Disc vs Diaphragm Couplings”, Machine Design, 24, 1986.

[9] Mancuso Jon R., “General purpose vs special purpose couplings”, Proceedings of the twenty-third turbomachinery symposium, 2001, pp167-177.

[10] Mancuso Jon R., Gibbons, C.B., et al. “The application of flexible coupling for turbomachinery”, Proceeding of the eighteenth turbomachinery symposium, Tutorial 1 on coupling, pp141-164.

[11] Stewart, Matthew J., Roberts, Kenneth G., et al. “Double Diaphragm Compound Shaft”, U.S. Patent #5,964,663, Oct. 1999.

[12] Stewart, Matthew J., Roberts, Kenneth G., et al. “Double Diaphragm Compound Shaft”, U.S. Patent #6,037,687, Mar. 2000.

[13] Lubell Daniel, Weissert Dennis, “Rotor And Bearing System For A Turbomachine”, U.S. Patent #7,112,036, B2. Sep. 2006.

[14] He Fubao, Shen Yapeng, “Plate and shell theory”, Xi’an, Xi’an Jiaotong University Press, 1993. (In Chinese)

[15] Xu Bingye, Liu Xinsheng, “Applied elastic and plastic mechanics”, Beijing, Tsinghua university press, 1995, pp237. (In Chinese)

[16] Liu Hongwen, “Material mechanics(edition4)”, Beijing, Senior educational press, 2005. (In Chinese)

## ANNEX A

**Table.1 Calculation parameters of the diaphragm coupling**

Parameters of the diaphragm coupling		Description	value
Items	Name		
Material Properties	$E$	Elastic Modulus	$115 \times 10^3 \text{ MPa}$
	$\mu$	Poisson's Ratio	0.3
	$\sigma_s$	Yield Limit	$825 \text{ MPa}$
	$n$	Safety Coefficient	1.2
Operating Conditions	$n_0$	Rotary Speed	$90000 \text{ rpm}$
	$P_0$	Input Power	130KW
Geometric Parameters	$h_1$	Thickness of the right diaphragm	1mm
	$r_{r2}$	Outer radius of the right diaphragm	12.5mm
	$h_2$	Thickness of the left diaphragm	1.2mm
	$r_{l2}$	Outer radius of the left diaphragm	17.5mm
	$r_0$	Radius of the middle shaft	4mm
	$l$	Length of the middle shaft	49mm
Additional Parameters	$\delta_r$	Deformation of the right diaphragm in the final equilibrium state considered effects from inertial forces and torque, but no misalignment	0.1mm
	$\delta_l$	Deformation of the left diaphragm in the final equilibrium state considered effects from inertial forces and torque, but no misalignment	0.104mm

## ANNEX B

**Flow Chart of The Solving Method and Steps**

